The 2018 hot drought pushed conifer wood formation to the limit of its plasticity : Consequences for woody biomass production and tree ring structure

E. Larysch, D F Stangler, H. Puhlmann, C B K Rathgeber, T. Seifert, H.-p. Kahle

HAL Id: hal-04226870
https://hal.inrae.fr/hal-04226870v1

Submitted on 3 Oct 2023

RESEARCH ARTICLE

The 2018 hot drought pushed conifer wood formation to the limit of its plasticity: Consequences for woody biomass production and tree ring structure

E. Larysch[1] (iD), D. F. Stangler[1], H. Puhlmann[2], C. B. K. Rathgeber[3,4], T. Seifert[1,5] & H.-P. Kahle[1]

1 Chair of Forest Growth and Dendroecology, Albert-Ludwigs-University, Freiburg, Germany
2 Department of Soil and Environment, Forest Research Institute Baden-Württemberg, Freiburg, Germany
3 INRAE, SILVA, Université de Lorraine, AgroParisTech, Nancy, France
4 Swiss Federal Research Institute for Forest, Snow and Landscape Research WSL, Birmensdorf, Switzerland
5 Department of Forest and Wood Science, Stellenbosch University, Matieland, South Africa

ABSTRACT

- Hot droughts are expected to increase in Europe and disturb forest ecosystem functioning. Wood formation of trees has the potential to adapt to those events by compensatory mechanisms between the rates and durations of tracheid differentiation to form the typical pattern of vital wood anatomical structures.
- We monitored xylogenesis and measured wood anatomy of mature silver fir (*Abies alba* Mill.) and Scots pine (*Pinus sylvestris* L.) trees along an elevational gradient in the Black Forest during the hot drought year of 2018. We assessed the kinetics of tracheid differentiation and the final tracheid dimensions and quantified the relationship between rates and durations of cell differentiation over the growing season.
- Cell differentiation kinetics were decoupled, and temperature and water availability signals were imprinted in the tree ring structure. The sudden decline in woody biomass production provided evidence for a disruption in carbon sequestration processes due to heat and drought stress. Growth processes of Scots pine (pioneer species) were mainly affected by the spring drought, whereas silver fir (climax species) growth processes were more disturbed by the summer drought.
- Our study provides novel insights on the plasticity of wood formation and carbon allocation in temperate conifer tree species in response to extreme climatic events.

INTRODUCTION

Climate change-induced extreme events, such as prolonged summer droughts or heatwaves, have become more frequent in recent years and are projected to increase in Central Europe (Füssel *et al.* 2017; Ionita & Nagavciuc 2021; Seneviratne *et al.* 2021). In Europe, growth and vigour of most tree species are already negatively affected by climate change (Eilmann *et al.* 2011; Weemstra *et al.* 2013; Vanoni *et al.* 2016; Archambeau *et al.* 2020; Buras *et al.* 2020; Lindner & Verkerk 2020; Schuldt *et al.* 2020; Charrier *et al.* 2021). To further sustain healthy and stable European forests, the tree species composition needs to be adapted to anticipated changes in environmental conditions (Aquilué *et al.* 2021; Messier *et al.* 2021). Due to their high productivity, versatile wood properties and high substitution potential for replacing non-renewable materials, coniferous tree species are considered key elements in forest management and the wood industry. Silver fir (*Abies alba* Mill.) and Scots pine (*Pinus sylvestris* L.) are considered relatively robust against drought (Reif *et al.* 2010; van der Maaten-Theunissen *et al.* 2013; Dolos & Märkel 2016; Meining *et al.* 2016), but detailed and comparative observations of the adaptive capacity of their intra-annual wood formation dynamics in response to extreme drought conditions are still scarce (Larysch *et al.* 2021).

The changes in growth dynamics under drought are often visible as reduced tree ring width, where fewer cells are being produced because of low cell division rates and/or premature cessation of cambial activity (Camarero *et al.* 2010; Gruber *et al.* 2010; Vieira *et al.* 2013; Ren *et al.* 2015), and in the wood anatomy, where the cell lumen and cell walls are abnormally altered compared to the expected cell morphology (Eilmann *et al.* 2011; de Micco *et al.* 2016). Under average climatic conditions, tree rings formed in conifer tree species are characterized by the genetically determined sequence from thin-walled, large tracheids produced in the early growing season to thick-walled tracheids with a narrow lumen produced in the late growing season (Fonti *et al.* 2010; Cuny *et al.* 2014). The process of wood formation (xylogenesis) for each tracheid cell follows consecutive differentiation phases, from cambial division, through radial cell enlargement, to cell wall thickening and lignification and, finally, to programmed cell death (Fromm 2013; Rathgeber *et al.* 2016). During cell differentiation, the rate and duration of the enlargement process results in the final size of the cell. In the subsequent phase of cell wall thickening and lignification (hereafter wall thickening), cell wall materials (cellulose, hemicellulose and lignin) are deposited in the secondary cell walls, which eventually consist of about 50% carbon (Lamlom & Savidge 2003). Through the process of cell

wall thickening, as the mechanism behind the woody biomass production, forests currently sequester up to 15% of the global annual anthropogenic CO_2 emissions. The process of cell wall thickening in xylogenesis is therefore essential for the carbon sink and storage capacity in forest ecosystems (Zhao & Running 2010; Pan 2011; Cuny *et al.* 2015).

During the differentiation phases of enlargement and wall thickening, the cell anatomy and the resulting tree-ring sequence are shaped and controlled by intrinsic and extrinsic factors (Balducci *et al.* 2016; Cuny & Rathgeber 2016; Cuny *et al.* 2019; de Micco *et al.* 2019; Rathgeber *et al.* 2019; Peters *et al.* 2021). Temperature influences the resumption of cambial activity (Begum *et al.* 2013; Delpierre *et al.* 2019), the onset of wood formation and many cellular metabolic processes, including the carbon allocation during wall thickening (Körner 2003; Rossi *et al.* 2008; Simard *et al.* 2013; Cuny *et al.* 2015). Water supply is an important resource for wood formation processes. Cell production and cell enlargement were observed to be negatively affected by water limitation, causing a reduction in turgor pressure, which plays a central role for the final tracheid dimensions (Cabon *et al.* 2020; Peters *et al.* 2021). Also, cell wall thickening is affected by turgor pressure, which must exceed a certain threshold for successful cell wall polysaccharide deposition (Hilty *et al.* 2021), and which passively influences the reallocation of sugars, which are usually deposited in the cell wall but are needed for osmotic purposes under water deficit (Pantin *et al.* 2013; Deslauriers *et al.* 2014a).

However, if environmental stress affects development of the endogenously predefined wood anatomical structure, compensatory mechanisms in wood formation kinetics take over (Balducci *et al.* 2016; Cuny & Rathgeber 2016; Garcia-Forner *et al.* 2019; Vieira *et al.* 2019, 2020; Stangler *et al.* 2021). Within the subprocesses of enlargement and wall thickening, rates and durations are tightly coupled and mutually balanced (Cuny *et al.* 2019). If the rates of enlargement or wall thickening decline, the corresponding durations of the cell differentiation phases adequately increase to compensate for these effects on the final cell anatomy (Balducci *et al.* 2016). Using these dynamic compensatory mechanisms, the plant is able to perform as usual after a disturbance, because the wood anatomical functions of water transport and mechanical stability remain largely unaffected by variations in weather and climate. Xylem cells must guarantee water transport to the crown by having a wide lumen and thin cell walls but must also physically support the tree through cells with thick cell walls and narrow lumens (Hacke & Sperry 2001). However, there is recent evidence that, under intense drought stress situations, these compensatory mechanisms fail, wood production becomes limited, and wood anatomy, thus the hydraulic system and the carbon stock of the tree are affected by environmental changes (Vieira *et al.* 2020; Stangler *et al.* 2021). It is still not fully known under which environmental conditions and at which time during the vegetation period the compensatory mechanisms can no longer function. A detailed evaluation of the kinetics of tracheid differentiation is crucial for quantification of a tree species performance and potential to resist and adapt to the impacts of weather extremes and environmental changes on wood formation. Our study aims to understand the effect of the hot drought year of 2018 on the kinetics of tracheid differentiation and seasonal dynamics of woody biomass production of silver fir and Scots pine growing along an elevational gradient in temperate climates. The hypotheses tested are: (i)

rates of cell differentiation are expected to be positively related to temperature; (ii) apart from the last cells, the duration of cell differentiation should be negatively related to temperature; (iii) because of water limitation, the rates of cell differentiation are expected to decrease and cell differentiation durations are expected to increase as a compensation, but the extent of this compensation might vary along the elevational gradient; (iv) seasonal dynamics of aboveground woody biomass production will generally follow the seasonal course of temperature. We assume strong variations from this pattern, including a premature decrease in woody biomass production under the hot drought conditions of 2018.

MATERIAL AND METHODS

Study site and sample tree selection

Close to the city of Freiburg (47° 59′ 41.38″ N, 7° 50′ 59.57″ E), in mature European beech and silver fir forest stands admixed with Scots pine (stand age 70 to 100 years), we established temporary sample plots along two elevational transects, each spanning four elevation levels (ca. 450 m, 650 m, 850 m and 1100 m a.s.l.). The climate type in the study area is a sub-Atlantic temperate climate. From the lowest to highest elevation, the gradient spans a 5° C mean annual temperature decrease and a 700 mm annual precipitation increase (baseline climate means for 1981–2010). On eight sample plots, we selected, in total, 42 dominant and co-dominant, vital sample trees of silver fir (24 trees) and Scots pine (18 trees), which showed no visible signs of crown or stem damage. At the highest elevation (1100 m a.s.l.), no Scots pine trees met the selection criteria. For details of weather conditions, study sites and the sample trees see Table S1 and Larysch *et al.* (2021).

Field and laboratory methods

Stem wood formation was assessed during the complete growing season from March to December 2018 by sampling microcores at breast height (1.3 m) at weekly to 10-day interval using the Trephor tool (Rossi *et al.* 2006). On site, the microcores were placed in Eppendorf microtubes in 50% ethanol solution. In the laboratory, the microcores were stored at 5° C to avoid tissue deterioration. For preparation, the microcores were dehydrated in stepwise increasing ethanol solutions and embedded in blocks of glycolmethacrylate (Heraeus Kulzer, Hanau, Germany). Approximately 1700 thin sections of 15–20 µm thickness were taken with a GSL-1 microtome, stained with cresyl violet acetate and permanently mounted with Euparal (Gärtner *et al.* 2014). All anatomical sections were analysed under a Nikon Eclipse Ni-E transmission light microscope (Nikon, Düsseldorf, Germany) to describe the temporal development of tracheid differentiation in each tree (see Figure S1). Therefore, tracheid development was tracked along three radial files in each tree, within each elevation site and at each sampling date by counting the number of cells in the cambial zone (nC), enlargement zone (nE), wall thickening zone (nW) and mature zone (nM). Cambial cells were identified as narrow cells with small radial diameters and thin primary cell walls. Enlarging cells are characterized as having a radial diameter at least twice that of the cambial cell radial diameter. Wall thickening cells were detected as semi-crystalline structures of

cellulose in secondary cell walls under polarized light. Mature, dead cells, have blue cell walls and no cell cytoplasm. Cell cytoplasm is self-digested through autolysis and disappears or is visibly defragmented after the autolysis is complete (Torrey et al. 1971). To measure wood anatomy and tracheid dimensions, we recorded a digital image (0.49 μm px^{-1}) of a thin section of an entire and fully differentiated tree ring after the vegetation period, and measured cell dimensions along five radial files in the tree ring of 2018 of each sample tree using the image analysis software ROXAS (von Arx & Carrer 2014; Prendin et al. 2017). From ROXAS images, for each cell (the cellular level was further characterized with subscript 'i') we characterized the wood anatomical variables cell lumen radial diameter (LRD$_i$), cell lumen tangential diameter (LTD$_i$), cell wall radial thickness (WRT$_i$), cell wall tangential thickness (WTT$_i$) and cell lumen cross-sectional area (LCA$_i$). We then calculated the cell cross-sectional area (CCA$_i$) as the product of cell radial and tangential diameter. The cell wall cross-sectional ares (WCA$_i$) as the final result of the wall thickening process was calculated by subtracting the cell lumen cross-sectional area from the cell cross-sectional area (see Table 1, Figure S2).

Quantitative analysis of wood formation and wood anatomy

All calculations and data analyses were performed in the R programming environment (R Core Team 2019). We used the R package RAPTOR to extract the tracheid files (Peters et al. 2018), smoothed the raw measurements of wood anatomical variables using generalized additive models (Wood 2017), and combined information on the timing of cell differentiation (wood formation) with its final geometry (wood anatomy) for each cell in each sample tree. To retain most of the detailed tree individual information, we decided to model the seasonal course of wood formation at the tree level, not at the stand level. The seasonal variation in cell number in each cell differentiation phase was modelled according to the procedure developed by Stangler et al. (2021) (see Figure S1). We then calculated the entry dates into cell enlargement (e$_i$E), cell wall thickening (e$_i$W) and cell maturity (e$_i$M), and the durations of each cell i in the cell differentiation phases of cell enlargement (d$_i$E = e$_i$W − e$_i$E) and cell wall thickening (d$_i$W = e$_i$M − e$_i$W) based on the approach of Cuny et al. (2013, 2014) (see Figure S3). The cell enlargement rate (r$_i$E) was calculated by dividing cell radial diameter [CRD$_i$ minus average cambial cell radial diameter (CCRD = 7 μm) directly after cambial cell division] by the residence time of the cell i in the enlargement phase (d$_i$E). The cell wall deposition rate (r$_i$W) was calculated by dividing the wall cross-sectional area [minus primary cell wall material of the cambial cell wall cross-sectional area (CWCA) built during cambial division] by residence time of the cell in the wall thickening phase. The rate of cell cross-sectional area enlargement (r$_i$A) was calculated by dividing cell cross-sectional area [minus cambium cell cross-sectional area (CCCA)] by duration of the enlargement. The xylem cell production rate (r$_t$CP) on day of year t was modelled by calculating the first order differences of the cumulative total number of xylem cells (n$_t$EWM) appearing in the developing tree ring. The daily rate of radial xylem growth (r$_t$RG) was calculated as the sum of the contributions of cell production and of cell enlargement. To calculate woody biomass production (WBP$_t$), we used the formulae to calculate woody biomass production described in Stangler et al. (2021) (see Table 1). This required the following parameters: form coefficient (F) of the stem, tree height (H), tree diameter at breast height (DBH), xylem apparent density (XAD$_t$ = cell wall proportion multiplied with estimated cell wall density

Table 1. Acquisition and calculation of variables of wood formation kinetics, wood anatomy and woody biomass production based on Andrianantenaina et al. (2019), Cuny et al. (2019) and Stangler et al. (2021).

notation	variable	unit	acquisition
LRD	Lumen radial diameter	μm	Measured
LTD	Lumen tangential diameter	μm	Measured
LCA	Lumen cross-sectional area	μm^2	Measured
WRT	Wall radial thickness	μm	Measured
WTT	Wall tangential thickness	μm	Measured
WCA	Wall cross-sectional area	μm^2	WCA$_i$ = CCA$_i$ − LCA$_i$
CRD	Cell radial diameter	μm	CRD$_i$ = LRD$_i$ + 2 × WRT$_i$
CTD	Cell tangential diameter	μm	CTD$_i$ = LTD$_i$ + 2 × WTT$_i$
CCA	Cell cross-sectional area	μm^2	CCA$_i$ = CRD$_i$ × CTD$_i$
MC	Mork's criterion	—	MC$_i$ = 4 × WRT$_i$/LRD$_i$
MD	Morphometric density	kg m^{-3}	MD$_i$ = 1509 × WCA$_i$/CCA$_i$
dE	Duration of cell enlargement	days	Calculated based on entry dates
dW	Duration of wall thickening	days	Calculated based on entry dates
rE	Rate of cell enlargement	μm day^{-1}	r$_i$E = (CRD$_i$ − CCRD)/d$_i$E
rW	Rate of wall thickening	μm^2 day^{-1}	r$_i$W = (WCA$_i$ − CWCA)/d$_i$W
rA	Rate of cross-sectional area enlargement	μm^2 day^{-1}	r$_i$A = (CCA$_i$ − CCCA)/d$_i$E
rCP	Rate of xylem cell production	cells day^{-1}	r$_t$CP = n$_t$EWM − n$_{t-1}$EWM
rRG	Rate of radial xylem growth	μm day^{-1}	r$_t$RG = r$_t$E × n$_t$E + r$_t$CP × CCRD
CP	Cell production	Cells	CP$_t$ = n$_t$EWM
RG	Radial growth	μm	RG$_t$ = $\sum_{t'=1}^{t}$ r$_{t'}$RG
WBP	Aboveground woody biomass production	gC tree^{-1}	WBP$_t$ = F × H × XAD$_t$ × CC × π/4 × [(DBH + 2 × RG$_t$)^2 − DBH^2]
rWBP	Rate of aboveground woody biomass production	gC tree^{-1} day^{-1}	r$_t$WBP = WBP$_t$ − WBP$_{t-1}$

See also main text for complete description of all variable abbreviations.

1.509 g cm^{-3}) and an assumed carbon concentration (CC) of 50% (Lamlom & Savidge 2003; Thomas & Martin 2012; Andrianantenaina et al. 2019). All used variables and their development are listed in Table 1.

Identification of weather phases during the drought year 2018

To identify sequential intra-seasonal periods with distinct weather conditions (called 'weather phases') in the drought year 2018, we used the relative plant available water content in the soil (RelWat), calculated using the LWF Brook90 model, as classification scheme. The water budget modelling was carried out using the process-oriented forest hydrological simulation model LWF-Brook90, which calculates the water budget of a one-dimensional, multi-layered soil profile with vegetation cover at daily resolution (Hammel & Kennel 2001; Federer et al. 2003). The hydraulic properties of individual soil layers were parameterized according to Mualem (1976) and van Genuchten (1980). Evapotranspiration was calculated using the approach of Shuttleworth & Wallace (1985), which differentiates between evaporation originating from the soil or snow cover and transpiration and interception from plant cover, using a conductivity model. The seasonal variation in leaf area index is an important controlling factor for distribution of the energy available for evaporation between soil and plant, according to the Lambert-Beer law. The water demand is covered by the individual soil layers depending on water availability and root distribution (actual transpiration, Ta). The LWF-Brook90 model requires meteorological input data at daily resolution [precipitation, temperature, radiation, water vapour pressure, wind speed, which were provided by the chair of physical geography at the University of Hamburg, using a 250 × 250m grid (Dietrich et al. 2019)]. We subtracted daily values of the RelWat in the year 2018 from the daily values of the mean long-term RelWat (1981–2010) and smoothed the resulting index using a generalized additive model (Wood 2017). By analysing major inflection points in the index, we were able to identify six weather phases in 2018 (Fig. 1):

1   Pre-drought: start of 2018 with a cold and moist late winter;

2   Spring drought development: several consecutive days without precipitation and mean temperatures 4° C above the long-term mean;

3   Spring drought release: a rainy and warm period between spring and summer drought;

4   Summer drought development: intense precipitation deficit (up to 21 days without rain) with hot temperatures;

5   Full summer drought: after the precipitation deficit the RelWat index has a negative plateau;

6   Summer drought release: summer drought is followed by a rainy period and refilling of the soil water volume towards the end of the year.

The spring and summer dry phases were characterized by above average temperatures, severe precipitation deficits compared to the average rainfall in the respective period and decreasing soil water availability and soil matrix potential (Table 2). The two drought releases were described by less intense negative, or even positive, precipitation anomalies. Furthermore, the summer drought development was characterized by reaching an absolute minimum potential relative soil water content, which was reached several days earlier at the lower elevations (see Figure S4).

Statistical analysis

The model kinetics were tested for species difference using the Wilcoxon rank sum test and for multiple comparisons along the elevational gradient using the Dunn rank sum test (Bauer 1972; Dinno 2017).

To adjust the temporal resolution of the environmental data, we aggregated the wood formation kinetics, woody biomass production rates and wood anatomical variables on a daily basis for each tree. The daily dynamics of the tree-level response variables (r_tE, r_tW, d_tE, d_tW, CCA_t, WCA_t, r_tRG, r_tWBP) for each species at the elevational level were smoothed using a generalized additive model with an automated knot selection procedure (Wood 2017). To evaluate the different effects of T and RelWat in each weather phase, we stratified the data according to species (two levels), our eight response variables and weather phases (five occurring in the vegetation period), giving a total of 2 × 8 × 5 (=80) datasets. We computed linear models with z-transformed
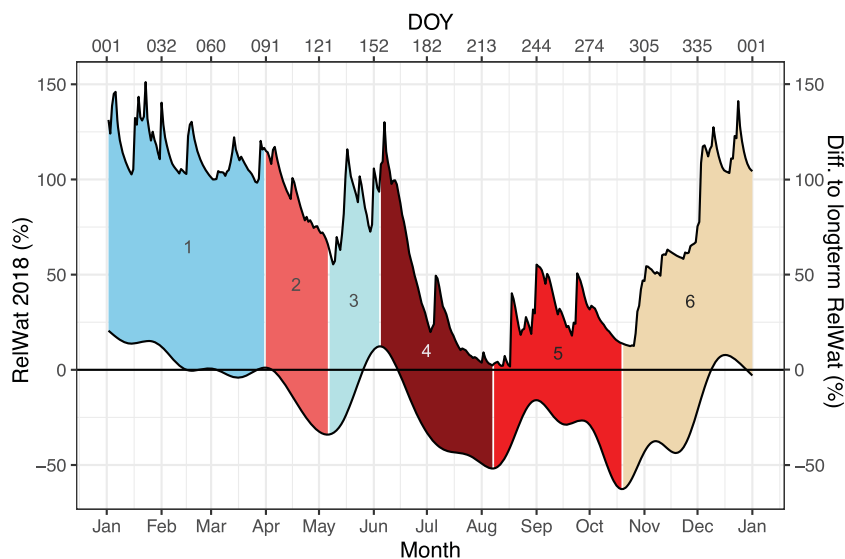
Fig. 1. Weather phases shown as coloured ribbons. (1) Pre-drought, (2) spring drought development, (3) spring drought release, (4) summer drought development, (5) summer sustained drought, (6) summer drought release. Upper curve represents daily relative plant available soil water content (RelWat %) in 2018 averaged over all the study sites. Lower curve represents the smoothed difference of the RelWat in 2018 to its long-term mean (1981–2010).

Table 2. Anomalies of precipitation sums (P) and air temperature (T), minimum relative soil water content (RelWat) and minimum soil matrix potential over the entire rooting zone (Psi) in the year 2018, for each weather phase.

| weather phase	ΔP [%]	ΔT [K]	min RelWat (%)	min Psi (kPa)
Predrought	+23%	−0.2	98.3%	−7.1
Spring: drought development	−65%	+4.2	66.0%	−46.1
Spring: drought release	+5%	+2.6	55.4%	−93.5
Summer: drought development	−45%	+2.1	2.3%	−1483.3
Summer: sustained drought	−35%	+1.9	1.7%	−1466.1
Summer: drought release	−19%	+0.9	12.4%	−1329.7

predictor variables T and RelWat for each response variable. To provide asymptotically valid inference in the presence of temporal autocorrelation, we applied bootstrapping to estimate confidence intervals and significance levels of the model coefficients by randomly selecting one day within each sample tree of each subsample. After bootstrapping the model 1000 times based on subsamples, we determined the significance of T and RelWat using the 90% (.), 95% (*), 99% (**) and 99.9% (***) percentile intervals of all bootstrapped coefficients. Furthermore, we calculated the variance inflation and R^2 of the model.

RESULTS

Cell structure development

The average cell cross-sectional area (CCA) gradually decreased in both species during the vegetation period of 2018 from about 1000 μm^2 to 250 μm^2 (Fig. 2a). The cells of silver fir were mostly larger compared to those of Scots pine until the summer solstice (Figure S5). All cell sizes decreased at the start of the drought, with variations between each elevational level. Most interestingly, cells in lower elevation Scots pine trees became smaller during the drought period and increased in size after the rain event in July, whereas cells at upper elevations were larger during drought compared to those at lower elevations (Fig. 2a). In silver fir CCA, there was no clear elevational trend.

The wall cross-sectional area (WCA) followed a unimodal course in silver fir and a bimodal course in Scots pine (Fig. 2b, Figure S5). After the start of the summer drought, Scots pine WCA moved from a steep increase to a steep decrease, with a further decrease in wall area during the whole period of precipitation deficit, having a turning point in mid-August, where WCA increased again for 2 weeks. Scots pine cell walls were smallest at the lowest elevation, with a positive trend along the gradient. Silver fir WCA also differed along the elevational gradient. WCA of the lowest elevation silver fir increased in spring and stopped shortly after the start of the precipitation deficit. The decrease in WCA was flat after the July rain event, after which there was a second strong decrease. The same pattern, but with less variation and generally smaller cell walls, can be seen in the second lowest elevation silver fir WCA. The uppermost elevation was synchronous with the lowest elevation, whereas the medium-high elevation had an intermediate role before strongly decreasing after the July rain event.
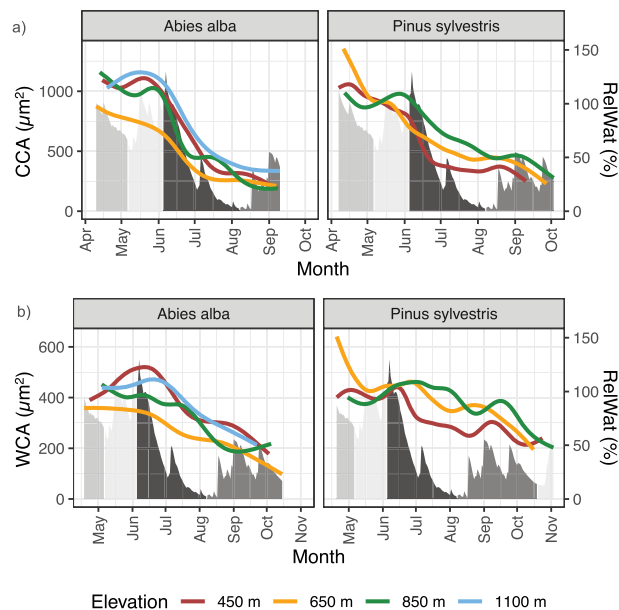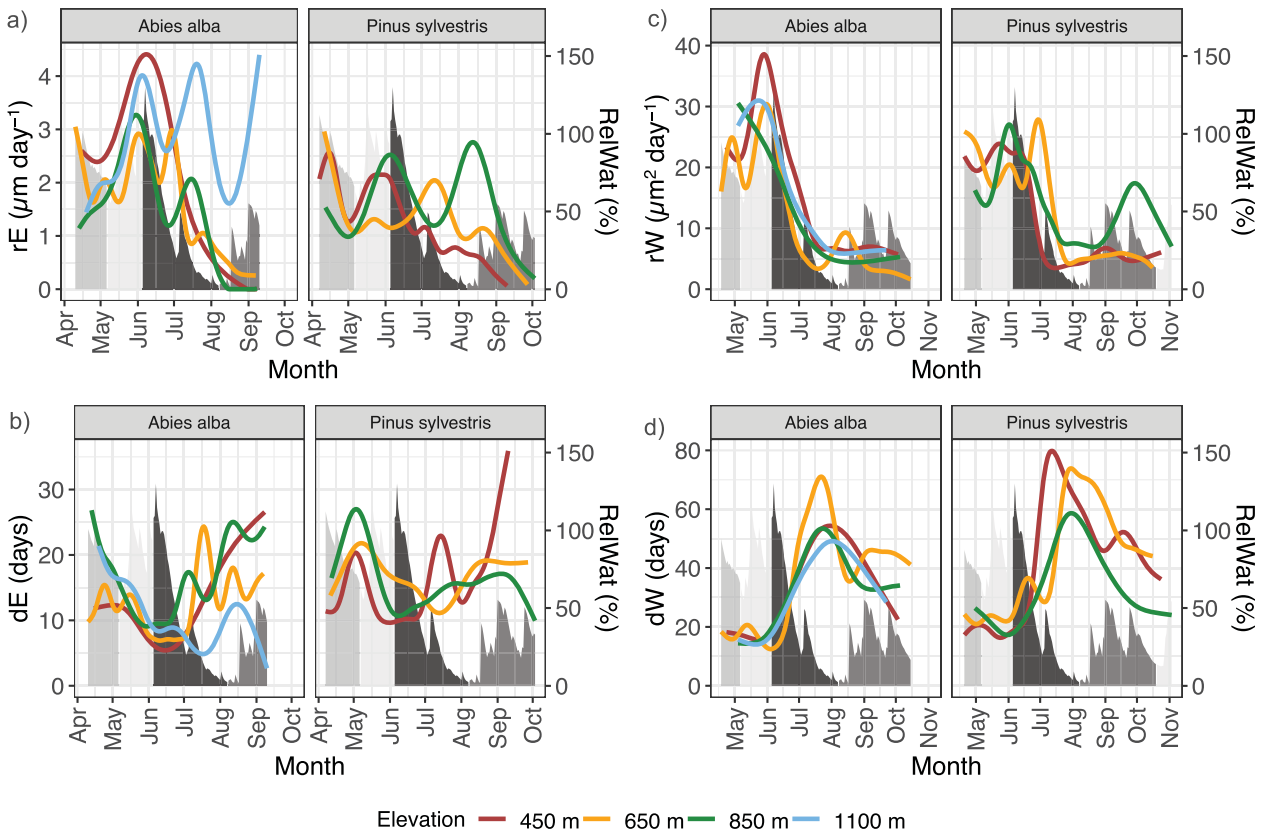

Fig. 2. Modelled daily dynamics of (a) cell cross-sectional area (CCA) and (b) wall cross-sectional area (WCA) of silver fir (left) and Scots pine (right) along the elevation gradient (red to blue), average weather phases (see Table 1), as shaded areas below, display average daily relative soil water amount (RelWat).

Daily course of wood formation kinetics

The lower elevation silver fir rate of enlargement (rE) decreased early during the spring drought, whereas the higher elevation silver fir rE increased, but with a lesser slope, at the end of the spring drought (Fig. 3a). During the spring drought release, silver fir rE strongly increased across all elevations. During development of the summer drought, the lower elevation silver fir rE fell rapidly and there was no recovery.

The higher elevation silver fir rE further increased again with the rainfall event in the first week of July. The lower elevation silver fir rE was not able to further increase after the rain event and fell further, whereas the highest elevation rE increased after minor rain events during the sustained summer drought. In Scots pine, rE dropped sharply during spring drought across all elevations (Fig. 3a) but the spring drought release allowed rE to recover best at the highest elevation. The drought with the intermittent rain events in July was directly visible at the lower elevation as a small local maximum, whereas the higher elevation Scots pine rE recovered slowly but the recovery was more pronounced.

The duration of enlargement (dE) in silver fir decreased until development of the summer drought, then plateaued until the rain event, after which all but the highest elevation dE increased (Fig. 3b). The uppermost elevation silver fir dE increased with decreasing rE. The dE at all elevations for Scots pine strongly increased during the spring drought, decreased during spring drought release and also maintained a low plateau with summer drought development (Fig. 3b). During the summer drought, the elevation signal was mixed. Throughout the vegetation period, silver fir dE was shortest at the lowest and uppermost elevations (Figure S6). Also, the average silver fir rE had a parabolic trend along the elevational gradient, with

Fig. 3. Modelled daily dynamics of (a) rate of enlargement (rE), (b) duration of enlargement (dE), (c) rate of wall thickening (rW), and (d) duration of wall thickening (dW) of silver fir (left) and Scots pine (right) along the elevation gradient (red to blue), average weather phases (see Table 1) as shaded areas below are average daily relative soil water amount (RelWat).

higher rates at the lowest and uppermost elevations compared to medium elevations, whereas Scots pine rE had no elevational trend (Figure S6). The xylem cells in silver fir increased in size, on average, at 2.51 µm day^{-1} for 11 days, while Scots pine xylem cells enlarged at a lower rate (−38%,1.56 µm day^{-1}) and needed, on average, 30% more time to fully enlarge (15.5 days). Only for 4 weeks during August was Scots pine rE higher, during the sharp decrease in silver fir rE, where Scots pine rE held the plateau for longer and decreased later (Figure S7).

On average, silver fir deposited cell wall material at a rate of 17.7 µm^2 day^{-1} and this was generally highest at the lowest elevation, whereas Scots pine deposited cell wall material at a significantly lower rate (−13%) and without an elevational trend. The development of the wall thickening rate (rW) was more uniform between the species and between elevations than the enlargement rate (Fig. 3c). During the spring drought, rW in Scots pine was already decreasing at all elevations, whereas in silver fir only the lower elevations started wall thickening and, thus, were the only elevations where rW decreased.

Across the elevational gradient, silver fir and Scots pine rW mostly increased during the spring drought release, peaked at the start of summer drought development and decreased drastically during the drought [from 30 µm^2 day^{-1} (fir) and 25 µm^2 day^{-1} (pine) to 5 µm^2 day^{-1}]. Only Scots pine rW at the high elevation recovered slightly (to 17 µm^2 day^{-1}) during the sustained drought. In silver fir, only at the second elevation

was a second local maximum (9.8 µm^2 day^{-1}) visible after the August rain event.

Along the elevational gradient, the course of the duration of wall thickening (dW) in silver fir was synchronous at every elevation except the medium-low elevation, where the intense increase of dW (similar to dE) did not respond to the July rain event but to the re-increase in rE during the sustained summer drought (Fig. 3d). Scots pine dW increased first and strongest at the lowest elevation during development of summer drought, whereas at the medium-high elevation there was a sharp increase of dW after the July rain event. The higher elevation Scots pine dW followed the average trend at a lower level (−5 to −10 days). Scots pine needed, on average, 18% longer (36 days) to fully synthesize cell wall material compared to silver fir (30 days). The shortest durations were recorded during spring drought release, and the highest durations occurred during summer drought, synchronous with the low rW (see also Figure S7).
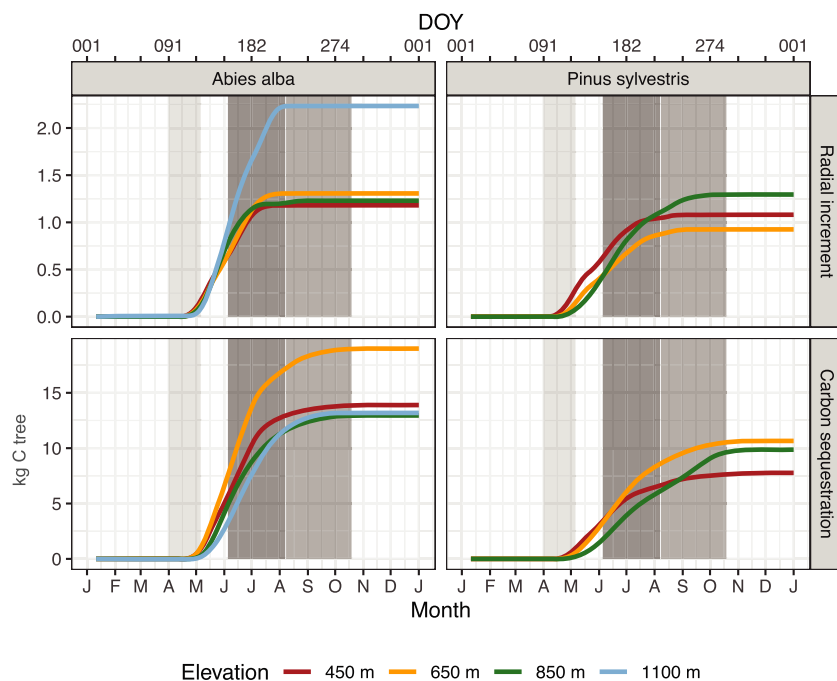
Dynamics of woody biomass production

Seasonal dynamics of the rate of tracheid cell production (rCP) in silver fir showed a unimodal pattern, with a simultaneous decrease at the start of the summer drought on 7 June. Scots pine rCP showed a bimodal pattern, with a local minimum during spring drought release at lower elevations and a second maximum in the second half of June (Fig. 4).
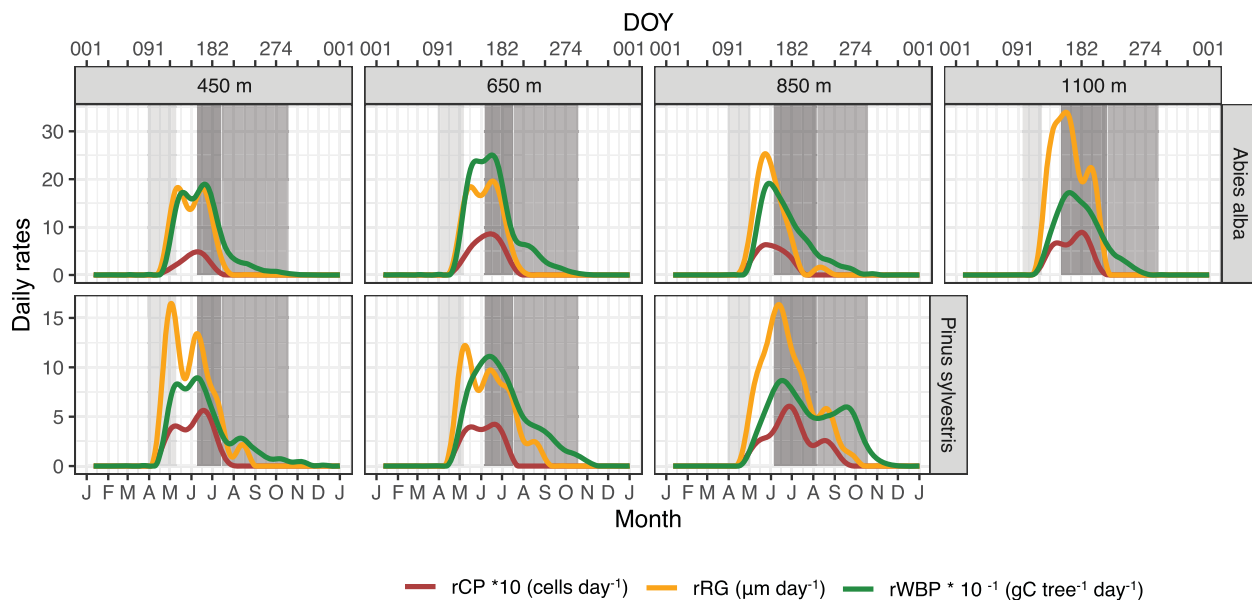
Fig. 4. Daily cell production rate (rCP), radial growth rate (rRG) and woody biomass production rate (rWBP) in silver fir (above) and Scots pine (below) along the elevation gradient (from left to right). Shaded areas are drought phases (see Table 1). For the purpose of illustration and comparison, rCP was multiplied by 10 and rWBP was divided by 10.

At the higher elevation (850 m), there was a second push in rCP in Scots pine, resulting in a prolongation of rCP. Silver fir stopped cell production and radial xylem increase after the precipitation deficit at all elevations. Silver fir rate of woody biomass production (rWBP) was much more pronounced compared to that of Scots pine. In both species, the maximum of rWBP occurred at the onset of summer drought development, simultaneously with rCP and rRG. Scots pine was able to re-increase rWBP after the rain event at the higher elevation. The cumulative radial increment curves revealed that at lower elevations silver fir

was more productive than Scots pine (Fig. 5). The carbon sequestration was considerably higher in silver fir than in Scots pine. Annual radial growth was maximum in silver fir at the highest elevation, whereas maximum carbon sequestration was reached on the second elevation, with 18.9 kg C tree^{-1} (Fig. 5). Also in Scots pine, the trees with the widest tree rings did not sequester the most carbon. The higher elevation Scots pine were able to increase carbon sequestration in the second part of the summer drought and they outcompeted the lower elevation trees in carbon accumulation during the summer drought.

Fig. 5. Modelled daily course of accumulated radial increment and accumulated aboveground woody biomass production during 2018 for silver fir (left) and Scots pine (right). Elevations are coloured from red to blue. Average weather phases (see Table 1) are shaded in grey.

Environmental effects in the enlargement process

During spring drought, the first weather phase in which the cambium was active, silver fir and Scots pine enlargement rates (rE) were positively stimulated by temperature and soil water content (Fig. 6a). During spring drought release, where soil water content was refilled, only temperature positively influenced rE. During summer drought development, silver fir rE was positively correlated with RelWat, which strongly decreased during this period. Scots pine rE was not significantly correlated with RelWat during summer drought.

During spring drought and the subsequent spring drought release, the duration of enlargement (dE) was negatively correlated with temperature in both species (Fig. 6b). Temperature and soil water content did not affect the durations of enlargement during the summer drought. The development of the cell cross-sectional area (CCA) in Scots pine was positively affected by temperature and soil water content during the spring drought, whereas the relationship of CCA with environment was unclear in silver fir (Fig. 6c). In the spring drought release, there was no visible connection between CCA and the environment. During summer drought development, CCA was considerably positively affected by RelWat for both species. Interestingly, during the summer drought plateau, CCA development no longer showed a significant effect of environment. The radial growth rate (rRG) in silver fir was positively
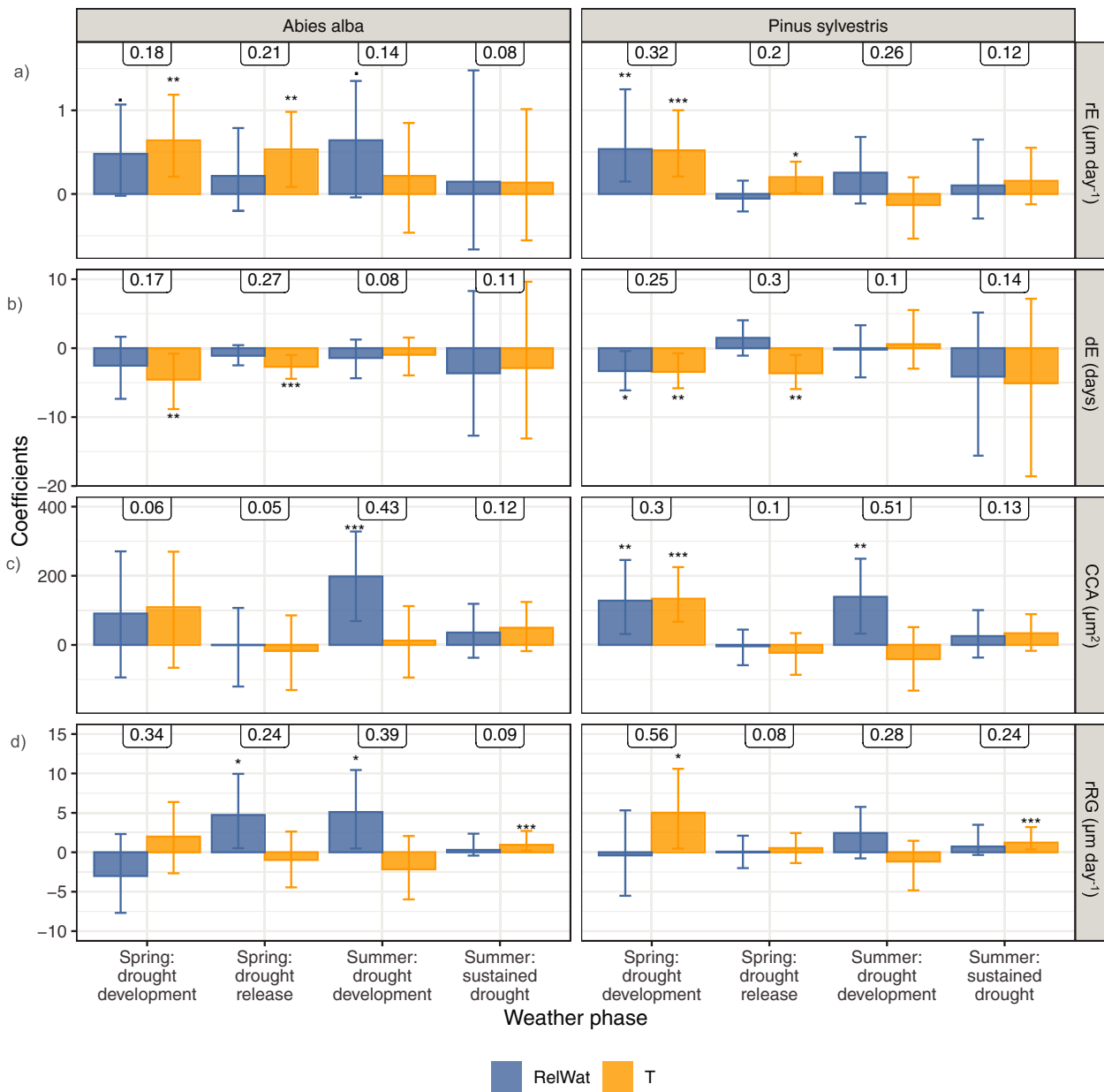
Fig. 6. Median and percentiles (2.5–97.5%) of bootstrapped coefficients of the linear model with responses of the cell enlargement process: (a) rate of cell enlargement, (b) duration of cell enlargement, (c) cell cross-sectional area, (d) rate of radial xylem growth. RelWat: relative plant available soil water content (%), T: Daily mean temperature (°C). Significance 90% ".", 95% "*", 99% "**", 99.9% "***". In black textbox R2.

stimulated by soil water in the spring drought release and in the summer drought development (Fig. 6d). During the summer drought, temperature positively affected silver fir rRG. Scots pine rRG was significantly affected by temperature during spring drought and the sustained summer drought.

Environmental effects in the wall thickening process

The rate of wall thickening (rW) remained largely unaffected during the spring, however Scots pine rW showed a slightly positive correlation with soil water content (Fig. 7a). During summer drought development, silver fir rW was negatively affected by soil water content but at a lesser intensity by temperature. During the subsequent drought plateau, the rW in silver fir continued to follow the course of temperature and soil water content. During summer drought development, Scots pine rW was also positively correlated with soil water content but without the additional temperature influence seen in silver fir. In both species, the late season rW was positively equally correlated to soil water and temperature. During summer drought development, the durations for depositing cell wall material (dW) were clearly and negatively affected by soil water; in silver fir already during spring drought release at a low intensity (Fig. 7b). During summer drought release, both soil water and temperature negatively affected dW at a high intensity. Scots pine wall cross-sectional area (WCA) was
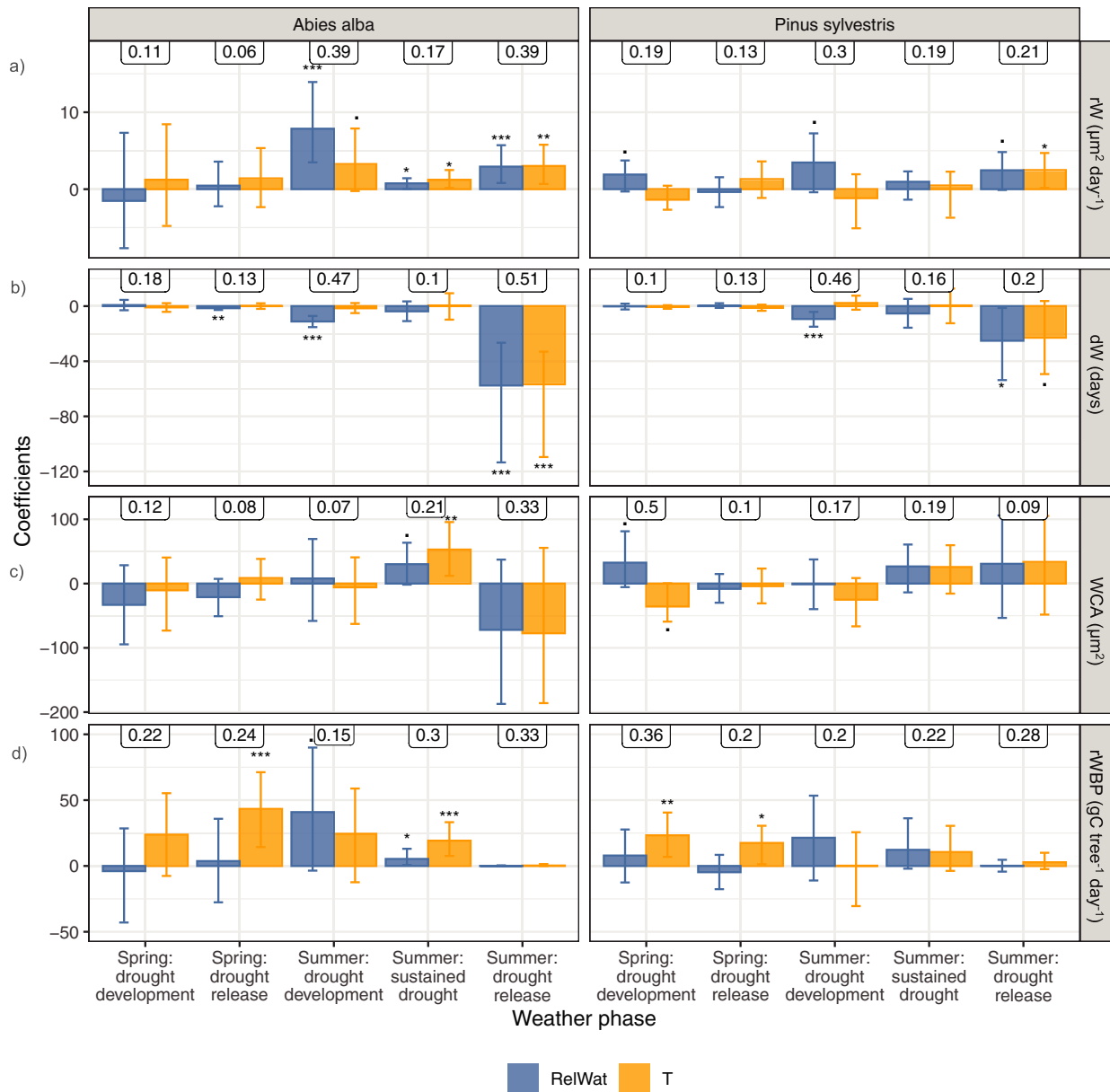

Fig. 7. Median and percentiles (2.5–97.5%) of bootstrapped coefficients of the linear model with responses of cell wall development: (a) rate of cell wall thickening, (b) duration of cell wall thickening, (c) cell wall cross-sectional area, (d) rate of aboveground woody biomass production. RelWat: relative plant available soil water content (%), T: Daily mean temperature (°C). Significance 90% ".", 95% "*", 99% "**", 99.9% "***". In black textbox R2.

positively affected by soil water and negatively affected by temperature during the spring drought (Fig. 7c). A tendency towards a negative influence of temperature was visible in Scots pine WCA during summer drought development. Silver fir WCA was not affected by environment in spring and was only positively correlated with soil water and temperature during the sustained summer drought. The influence of the environment on the rate of woody biomass production (rWBP) was higher in silver fir than in Scots pine (Fig. 7d). Silver fir rWBP was strongly and positively affected by temperature during spring drought release. Similarly, but at a less significant intensity, soil water positively affected rWBP during the summer drought development. In addition to the soil water impact, also temperature affected rWBP during the subsequent summer drought plateau. In Scots pine, temperature positively affected rWBP only during spring. In the summer drought release, there was no environmental influence detected in rWBP.

DISCUSSION

Cell enlargement and resulting cell size were differently affected by spring and summer droughts

Under non-extreme conditions, variations in soil water status neither relate to enlargement kinetics nor to the final cell dimensions (Cuny & Rathgeber 2016). Exceptional spring droughts can negatively impact tree ring width (Lebourgeois et al. 2010; George et al. 2015). In our study, the cell enlargements of silver fir and Scots pine were differently affected by the 2018 spring drought, and the effects also differed along the elevation gradient. Not only general climatic shifts can be seen along the elevation gradient, but also the severity of the drought (lower intensity coupled with faster recovery of soil water status with increasing elevation) and the intensity of the heat (less hot days with increasing elevation) is decreasing with increasing elevation (Čufar et al. 2012; Saderi et al. 2019; Miller et al. 2020; Larysch et al. 2021). During the spring drought, Scots pine strongly reduced cell enlargement rates at all elevations, whereas silver fir only reduced enlargement at lower elevations. Scots pine enlargement kinetics appeared partly decoupled, as the durations were not adequately extended to completely buffer the reduced rates, ergo there was not enough time to fully enlarge the tracheids, resulting in a negative impact on cell size even at the start of the growing season. Furthermore, the moderated cell production rate and the atypical accumulation of incomplete cells in the enlargement reservoir, which was depleted as soon as the soil water conditions improved, emphasize the drought effect on cell enlargement and the climate sensitivity of Scots pine, especially in response to spring water status (Oberhuber et al. 1998; Cuny et al. 2013; Figure S1). Silver fir radial growth at higher elevations was less disturbed, probably due to later growth onset and better site conditions during the hot drought. This is in line with the findings of Cabon et al. (2020b) and Stangler et al. (2021), who detected moderated responses of xylogenesis at high elevations to water limitations. The difference in stress tolerance could point to the life strategies of the two tree species. Scots pine, as a pioneer species, follows a risky life strategy, already producing more enlarging cells in spring than silver fir (Figure S1), which probably led to higher susceptibility to a drop in turgor pressure (Cuny et al. 2012; Peters et al. 2021; Cabon et al. 2020a).

The low turgor pressure, resulting from decreasing water supply and heat surplus of 4K, is often considered a major trigger for a reduction in tracheid expansion (Steppe et al. 2006; Balducci et al. 2016; Peters et al. 2021). In silver fir, the reduced rates in spring were compensated by prolonged durations of tracheid cell enlargement to their final dimensions, emphasizing tight coupling of the enlargement kinetics (Balducci et al. 2016; Cuny et al. 2019; Vieira et al. 2020). The successful compensation for reduced rates is visible in silver fir cell cross-sectional area, which was not affected by the spring drought. The enlargement process in silver fir was most intensely disturbed during summer drought development, comprising a 3-week precipitation deficit and a heat surplus of more than 2K, where enlargement rates strongly decreased. This decline was not fully buffered by increasing duration, leading to the decoupling of enlargement kinetics in silver fir, as visible in the accumulation of cells in the enlargement reservoir and in the significant positive relationship of cell size with soil water. Under severe drought stress, numerous tree species, e.g. black spruce, maritime pine, European beech and oak, are able to immediately react to improved water availability through high plasticity of cell production and wood formation processes (Balducci et al. 2013; Carvalho et al. 2015; Vanhellemont et al. 2019; Vieira et al. 2019). Also, Dietrich & Kahmen (2019) observed the benefit of low amounts of intermittent rainfall under drought conditions, which lead to mitigation of drought stress in trees. After the spring drought, both species showed the capacity to quickly react to better growing conditions, where water availability no longer influenced cell enlargement and rates increased, leading to decreased durations. During droughts, even small intermittent rain events can stop in the downward trend in the enlargement rate of Scots pine, and a second small increase in silver fir, in turn, leading to a flattened negative trend in cell size. This emphasizes the highly plastic responses of wood formation in conifers to extreme environmental conditions (Montwé et al. 2014; Nabais et al. 2014; Stangler et al. 2021).

Environmental control of wall thickening and carbon sequestration

We found major declines in wall thickening rates in response to environmental stress during spring and summer droughts. In contrast to the highly plastic enlargement process, the wall thickening dynamics followed a more stringent course, not responding to smaller drought-intermittent rain events. The decline in wall thickening rates was possibly initiated by altered cell wall polysaccharide allocation during drought, where sugars are prioritized for osmotic purposes, and maintenance of living tissues is more crucial for tree survival than growth during extreme stress events (Pantin et al. 2013; Deslauriers et al. 2014b; Cartenì et al. 2018). To overcome the limited availability of carbon and assure fully functional cell wall dimensions at the same time, the low wall thickening rates were compensated by extended durations. This tight coupling in wall thickening kinetics led to successful cell wall area development without imprinting environmental signals during most of the vegetation period, as also observed in other studies (Balducci et al. 2016; Cuny et al. 2019; Vieira et al. 2020). Nevertheless, similar to our findings on cell enlargement kinetics, in the wall thickening process we could identify a failure of

compensation mechanisms with different species-specific temporal stress sensitivity. In Scots pine, cell wall area was negatively affected by declining water supply and excess temperatures already during the spring drought, which led to declining rates that could not be compensated for because the durations stagnated. This underpins our hypothesis that Scots pine, as a pioneer species with a risky life strategy, is immediately stressed during a hot drought at the start of its growth period, where a sufficient water supply is vital for depositing cell wall material (Lebourgeois et al. 2010; Cuny et al. 2012). Silver fir cell wall area was negatively affected by the sustained summer drought, where both wall thickening and durations declined for several weeks (Figure S8). Also in Scots pine at low and medium elevations, such declines in duration started in the middle of the vegetation period and continued for weeks. A decoupling of compensatory mechanisms was also detected during latewood formation, where positive effects of temperature on wall thickening rates were not counterbalanced by decreased durations (Cuny & Rathgeber 2016; Stangler et al. 2021). In both species, the cell wall area declined throughout the growing period, in contrast to the endogenous course of cell morphology along the tree ring. In previous studies, decreasing cell wall dimensions were found to be a stress signal under chronic droughts (Eilmann et al. 2011; Martin-Benito et al. 2017; Vieira et al. 2020) and considered a result of decoupling (Vieira et al. 2020). We detected strong signals of low water supply in the cell wall area already during the spring drought in Scots pine. In silver fir, the cell wall area was only marginally affected by low soil moisture or high temperatures compared to the immediate impact of the environment on the wall thickening rate during summer drought development. Interestingly, cell wall dimensions were affected in the subsequent sustained summer drought phase, resulting in cells with a reduced cell wall cross-section area. To mitigate drought-induced cavitation, increasing cell wall thickness in relation to cell size has often been found to be an effective strategy (Hacke & Sperry 2001). However, it seems that in both species, cell wall formation must react to the drought-induced alterations in the preceding enlargement process and to the carbon imbalance in order to maintain water transport, despite the increasing risk of cavitation. Fewer cells were produced under drought, thus reducing the conductive area available for water transport. Moreover, the produced cells were likely smaller because of the low turgor pressure during periods of tree water deficit. Nevertheless, the cell lumen and conductive area probably need to be kept large enough to ensure successful water transport, while potentially increasing the risk of embolism (Yin & Bauerle 2017). Eilmann et al. (2009) also reported that Scots pine responded to drought by producing a carbon efficient wood structure composed of cells with thin cell walls to potentially increase conductivity. In addition to the effects of xylem hydraulics, the immediate re-allocation of carbon (sink activity) and/or depletion of the carbon pool through reduced availability of photoassimilates (source activity) possibly mitigated the cell wall area decline (Gessler & Grossiord 2019).

Under normal climate conditions, the seasonal dynamics of woody biomass production follows a symmetrical bell-shaped course, similar to the temperature course in the Northern Hemisphere (Cuny et al. 2015). Confirming our proposal, we detected a deviation from the norm, which was visible in the bell-shaped right-skewed curve of the daily rates of aboveground woody biomass production, as also found by Andrianantenaina et al. (2019) during the drought year of 2015. Moreover, the woody biomass production rate revealed bimodal patterns at lower elevations and was immediately and strongly affected by the summer drought, being more intense in silver fir than in Scots pine. Intra-seasonal drought was found to temporally reduce woody biomass production in Norway spruce (Stangler et al. 2021). In Mediterranean regions, bimodal growth patterns are documented in response to the annual and repeated summer droughts (Camarero et al. 2010; Pacheco et al. 2018; Garcia-Forner et al. 2019). The premature decline in carbon sequestration, parallel to the decline in the xylem size increment, despite the successful coupling of wall thickening kinetics, led to the assumption that although the compensation mechanism functioned correctly, carbon sequestration was inhibited due to environmental constraints. This was already predicted in forest ecosystem productivity models following the 2003 drought and heatwave in European forests (Ciais et al. 2005).

Interestingly, the woody biomass production rate, as well as the wall deposition rate, in Scots pine at high elevation visibly increased after the August rain event. We interpret this re-increase as an advantage in Scots pine, which profited from the improvement in late growing conditions, as corroborated by the positive temperature stimulus and synchronous cell wall area increment, especially at the higher elevation, where cambial activity lasted longest (Larysch et al. 2021). This is in line with previous findings, where Scots pine maintained high xylogenetic plasticity (Cuny et al. 2012; Jyske et al. 2014; del Castillo et al. 2018; Vieira et al. 2019). Even if the wall thickening rates were generally synchronous across species, silver fir sequestered more carbon in the cell walls than Scots pine, similar to findings without climate constraints (Cuny et al. 2015). Scots pine maintains high plasticity in wood formation but low productivity and low carbon sequestration potential, as also documented by Bouriaud & Popa (2009). In global climate scenario models, only alpine regions are regarded as suitable habitat for Scots pine trees in the future, but also there Scots pine is largely suffering from drought (Bigler et al. 2006; Bombi et al. 2017; Archambeau et al. 2020).

The environmental imprint in the last cell lines

As postulated, we found that cell differentiation rates were positively influenced by air temperature and the durations of cell differentiation, except for the final latewood cells, which were negatively influenced by air temperature. The enlargement kinetics of the last latewood cells were neither clearly affected by late summer temperatures nor by soil water content, which could be translated as strong endogenous control of cell enlargement of the last-produced cells, in accordance with previous findings (Cuny et al. 2019). Interestingly, we observed a close relationship between the environment and the cell wall thickening kinetics during development of these last cells produced. In our study, cell wall material deposition rates of these last-developed cells were positively influenced by high temperatures, as also observed by Cuny & Rathgeber (2016). In addition, cell wall thickening was positively influenced by recovering soil water status with equally high intensity but higher variance explanation than temperature, emphasizing the imprinting of not only temperature but also water availability in the anatomy of the last-maturing cells.

CONCLUSION

Our study is the first to model wood formation kinetics of temperate forest tree species in a hot drought year. In addition to the well-known and previously documented effect of temperature (Cuny & Rathgeber 2016; Cuny *et al.* 2019), we demonstrate that the kinetics of wood formation and rates of carbon sequestration in conifers are also directly and significantly controlled by water availability during a year with an extreme hot summer drought. The strong decoupling in the wood formation kinetics, the environmental signals in cell dimensions and the abrupt decline in woody biomass production provide evidence for a disruption in wood formation and carbon sequestration processes because of a combination of repeated heat and drought stress during the growing season. Growth processes of Scots pines (a pioneer species) were mainly affected by the spring drought, whereas silver firs (a climax species) were more disturbed by the summer drought. We conclude that less drought-tolerant tree species will be at increased risk, especially on low elevation sites. Our results enable a more detailed understanding of the impact of complex hot droughts on temperate conifer forest productivity and carbon sequestration. In addition, our study provides novel insights into contrasting carbon allocation strategies of a pioneer and a climax conifer tree species.

ACKNOWLEDGEMENTS

SUPPORTING INFORMATION

Additional supporting information may be found online in the Supporting Information section at the end of the article.

Table S1. Average temperature and precipitation sum and the 2018 deviance, species mean diameter at breast height (DBH), mean height (H) and mean tree age at each elevation.

Figure S1. Modelled daily course of cell numbers in each cell differentiation phase (CZ cambial cells, EZ enlarging cells, WZ wall thickening cells, MZ mature cells) per elevation and species. Grey shaded areas represent the drought phases in 2018 (spring drought, summer precipitation deficit and sustained summer drought).

Figure S2. Cell cross-sectional area (CCA) and wall cross-13 sectional area (WCA) of each developed xylem cell of each study tree, modelled (GAM) over 5 measured tracheid rows in 2018 (k1, k2, k3 = Scots pine sample trees, t1, t2, t3 = silver fir sample trees on low sites G,S (450 m), medium-low sites U,W (650 m), medium-high sites H,B (850 m) and the high sites (1100 m).

Figure S3. Calculated durations of enlargement and wall thickening for e 18 ach developed xylem cell of each study tree (k1, k2, k3 = Scots pine sample trees, t1, t2, t3 = silver fir sample trees on low sites G,S (450 m), medium-low sites U,W (650 m), medium-high sites H,B (850 m) and the high sites (1100 m).

Figure S4. Relative soil water content (RelaWat, 0 = 0%, 1 = 100%) for each elevation (a) 450m, (b) 650m, (c) 850m, (d) 1100 m, weather phases colored as area below 2018 daily RelWat, black curve represents smoothed difference of the 2018 RelWat to the long-term mean RelWat (1981–2010).

Figure S5. Modelled (GAM) daily dynamics of (a) cell cross-sectional area (CCA) and (b) wall cross sectional area (WCA) of silver fir (green) and Scots pine (blue), weather phases (see T1) as shaded area below RelWat.

Figure S6. Boxplots of the wood formation kinetics of each elevational level (coloured) for each species. Different letters indicate significant contrast due to the Dunn rank sum test within each species (alpha level 0.05).

Figure S7. Modelled (GAM) daily dynamics of (a) rate of enlargement (rE), (b) the duration of enlargement (dE), (c) the rate of wall thickening (rW), and (d) the duration of wall thickening (dW) of silver fir (green) and Scots pine (blue), weather phases (see Table 1) as shaded area below RelWat.

Figure S8. Juxtaposition of enlargement and of wall thickening kinetics per species.

REFERENCES

Andrianantenaina A.N., Rathgeber C.B.K., Pérez-de-Lis G., Cuny H., Ruelle J. (2019) Quantifying intra-annual dynamics of carbon sequestration in the forming wood: a novel histologic approach. *Annals of Forest Science*, 76. https://doi.org/10.1007/s13595-019-0846-7

Aquilué N., Messier C., Martins K.T., Dumais-Lalonde V., Mina M. (2021) A simple-to-use management approach to boost adaptive capacity of forests to global uncertainty. *Forest Ecology and Management*, 481, 118692. https://doi.org/10.1016/j.foreco.2020.118692

Archambeau J., Ruiz-Benito P., Ratcliffe S., Fréjaville T., Changenet A., Muñoz Castañeda J.M., Lehtonen A., Dahlgren J., Zavala M.A., Benito Garzón M.

(2020) Similar patterns of background mortality across Europe are mostly driven by drought in European beech and a combination of drought and competition in Scots pine. *Agricultural and Forest Meteorology*, 280, 107772. https://doi.org/10.1016/j.agrformet.2019.107772

von Arx G., Carrer M. (2014) Roxas—a new tool to build centuries-long tracheid-lumen chronologies in conifers. *Dendrochronologia*, 32(3), 290–293. https://doi.org/10.1016/j.dendro.2013.12.001

Balducci L., Cuny H.E., Rathgeber C.B.K., Deslauriers A., Giovannelli A., Rossi S. (2016) Compensatory mechanisms mitigate the effect of warming and drought on wood formation. *Plant, Cell & Environment*, 39, 1338–1352. https://doi.org/10.1111/pce.12689

Balducci L., Deslauriers A., Giovannelli A., Rossi S., Rathgeber C.B.K. (2013) Effects of temperature and

water deficit on cambial activity and woody ring features in *Picea mariana* saplings. *Tree Physiology*, 33, 1006–1017. https://doi.org/10.1093/treephys/tpt073

Bauer D.F. (1972) Constructing confidence sets using rank statistics. *Journal of the American Statistical Association*, 67, 687–690. https://doi.org/10.1080/01621459.1972.10481279

Begum S., Nakaba S., Yamagishi Y., Oribe Y., Funada R. (2013) Regulation of cambial activity in relation to environmental conditions: understanding the role of temperature in wood formation of trees. *Physiologia Plantarum*, 147, 46–54. https://doi.org/10.1111/j.1399-3054.2012.01663.x

Bigler C., Bräker O.U., Bugmann H., Dobbertin M., Rigling A. (2006) Drought as an inciting mortality factor in Scots pine stands of the Valais, Switzerland.

Ecosystems, **9**, 330–343. https://doi.org/10.1007/s10021-005-0126-2

Bombi P., D'Andrea E., Rezaie N., Cammarano M., Matteucci G. (2017) Which climate change path are we following? Bad news from Scots pine. *PLoS One*, **12**, e0189468. https://doi.org/10.1371/journal.pone.0189468

Bouriaud O., Popa I. (2009) Comparative dendroclimatic study of Scots pine, Norway spruce, and silver fir in the Vrancea Range, Eastern Carpathian Mountains. *Trees—Structure and Function*, **23**, 95–106. https://doi.org/10.1007/s00468-008-0258-z

Buras A., Rammig A., Zang C.S. (2020) Quantifying impacts of the 2018 drought on European ecosystems in comparison to 2003. *Biogeosciences*, **17**, 1655–1672. https://doi.org/10.5194/bg-17-1655-2020

Cabon A., Fernández-de-Uña L., Gea-Izquierdo G., Meinzer F.C., Woodruff D.R., Martínez-Vilalta J., De Cáceres M. (2020a) Water potential control of turgor-driven tracheid enlargement in Scots pine at its xeric distribution edge. *New Phytologist*, **225**(1), 209–221. https://doi.org/10.1111/nph.16146

Cabon A., Peters R.L., Fonti P., Martínez-Vilalta J., De Cáceres M. (2020b) Temperature and water potential co-limit stem cambial activity along a steep elevational gradient. *New Phytologist*, **226**, 1325–1340. https://doi.org/10.1111/nph.16456

Camarero J.J., Olano J.M., Parras A. (2010) Plastic bimodal xylogenesis in conifers from continental Mediterranean climates. *New Phytologist*, **185**, 471–480. https://doi.org/10.1111/j.1469-8137.2009.03073.x

Cartenì F., Deslauriers A., Rossi S., Morin H., De Micco V., Mazzoleni S., Giannino F. (2018) The physiological mechanisms behind the earlywood-to-latewood transition: a process-based modeling approach. *Frontiers in Plant Science*, **9**. https://doi.org/10.3389/fpls.2018.01053

Carvalho A., Nabais C., Vieira J., Rossi S., Campelo F. (2015) Plastic response of Tracheids in *Pinus pinaster* in a water-limited environment: adjusting lumen size instead of wall thickness. *PLoS One*, **10**, e0136305. https://doi.org/10.1371/journal.pone.0136305

Charrier G., Martin-StPaul N., Damesin C., Delpierre N., Hänninen H., Torres-Ruiz J.M., Davi H. (2021) Interaction of drought and frost in tree ecophysiology: rethinking the timing of risks. *Annals of Forest Science*, **78**, 1–15. https://doi.org/10.1007/s13595-021-01052-5

Ciais P.H., Reichstein M., Viovy N., Granier A., Ogée J., Allard V., Aubinet M., Buchmann N., Bernhofer C., Carrara A., Chevallier F., De Noblet N., Friend A.D., Friedlingstein P., Grünwald T., Heinesch B., Keronen P., Knohl A., Krinner G., Loustau D., Manca G., Matteucci G., Miglietta F., Ourcival J.M., Papale D., Pilegaard K., Rambal S., Seufert G., Soussana J.F., Sanz M.J., Schulze E.D., Vesala T., Valentini R. (2005) Europe-wide reduction in primary productivity caused by the heat and drought in 2003. *Nature*, **437**, 529–533. https://doi.org/10.1038/nature03972

Čufar K., De Luis M., Saz M.A., Črepinšek Z., Kajfež-Bogataj L. (2012) Temporal shifts in leaf phenology of beech (*Fagus sylvatica*) depend on elevation. *Trees*, **26**, 1091–1100. https://doi.org/10.1007/s00468-012-0686-7

Cuny H.E., Fonti P., Rathgeber C.B.K., Arx G., Peters R.L., Frank D.C. (2019) Couplings in cell differentiation kinetics mitigate air temperature influence on conifer wood anatomy. *Plant, Cell & Environment*, **42**, 1222–1232. https://doi.org/10.1111/pce.13464

Cuny H.E., Rathgeber C.B.K., Lebourgeois F., Fortin M., Fournier M. (2012) Life strategies in intra-annual dynamics of wood formation: example of three conifer species in a temperate forest in north-east France. *Tree Physiology*, **32**, 612–625. https://doi.org/10.1093/treephys/tps039

Cuny H.E., Rathgeber C.B.K., Kiessé T.S., Hartmann F.P., Barbeito I., Fournier M. (2013) Generalized additive models reveal the intrinsic complexity of wood formation dynamics. *Journal of Experimental Botany*, **64**, 1983–1994. https://doi.org/10.1093/jxb/ert057

Cuny H.E., Rathgeber C.B.K., Frank D., Fonti P., Fournier M. (2014) Kinetics of tracheid development explain conifer tree-ring structure. *New Phytologist*, **203**, 1231–1241. https://doi.org/10.1111/nph.12871

Cuny H.E., Rathgeber C.B.K., Frank D., Fonti P., Mäkinen H., Prislan P., Rossi S., del Castillo E.M., Campelo F., Vavrčík H., Camarero J.J., Bryukhanova M.V., Jyske T., Gričar J., Gryc V., De Luis M., Vieira J., Čufar K., Kirdyanov A.V., Oberhuber W., Treml V., Huang J.-G., Li X., Swidrak I., Deslauriers A., Liang E., Nöjd P., Gruber A., Nabais C., Morin H., Krause C., King G., Fournier M. (2015) Woody biomass production lags stem-girth increase by over one month in coniferous forests. *Nature Plants*, **1**, 15160. https://doi.org/10.1038/nplants.2015.160

Cuny H.E., Rathgeber C.B.K. (2016) Xylogenesis: coniferous trees of temperate forests are listening to the climate tale during the growing season but only remember the last words! *Plant Physiology*, **171**, 306–317. https://doi.org/10.1104/pp.16.00037

De Micco V., Campelo F., De Luis M., Bräuning A., Grabner M., Battipaglia G., Cherubini P. (2016) Intra-annual density fluctuations in tree rings: how, when, where, and why? *IAWA Journal*, **37**, 232–259. https://doi.org/10.1163/22941932-20160132

De Micco V., Carrer M., Rathgeber C.B.K., Julio Camarero J., Voltas J., Cherubini P., Battipaglia G. (2019) From xylogenesis to tree rings: wood traits to investigate tree response to environmental changes. *IAWA Journal*, **40**, 2–29. https://doi.org/10.1163/22941932-40190246

Delpierre N., Lireux S., Hartig F., Camarero J.J., Cheaib A., Čufar K., Cuny H., Deslauriers A., Fonti P., Gričar J., Huang J.-G., Krause C., Liu G., de Luis M., Mäkinen H., del Castillo E.M., Morin H., Nöjd P., Oberhuber W., Prislan P., Rossi S., Saderi S.M., Treml V., Vavrick H., Rathgeber C.B.K. (2019) Chilling and forcing temperatures interact to predict the onset of wood formation in Northern Hemisphere conifers. *Global Change Biology*, **25**, 1089–1105. https://doi.org/10.1111/gcb.14539

Deslauriers A., Beaulieu M., Balducci L., Giovannelli A., Gagnon M.J., Rossi S. (2014a) Impact of warming and drought on carbon balance related to wood formation in black spruce. *Annals of Botany*, **114**, 335–345. https://doi.org/10.1093/aob/mcu111

Deslauriers A., Beaulieu M., Balducci L., Giovannelli A., Gagnon M.J., Rossi S. (2014b) Impact of warming and drought on carbon balance related to wood formation in black spruce. *Annals of Botany*, **114**, 335–345. https://doi.org/10.1093/aob/mcu111

Dietrich H., Wolf T., Kawohl T., Wehberg J., Kändler G., Mette T., Röder A., Böhner J. (2019) Temporal and spatial high-resolution climate data from 1961 to 2100 for the German National Forest Inventory (NFI). *Annals of Forest Science*, **76**, 6. https://doi.org/10.1007/s13595-018-0788-5

Dietrich L., Kahmen A. (2019) Water relations of drought-stressed temperate trees benefit from short drought-intermitting rainfall events. *Agricultural and Forest Meteorology*, **265**, 70–77. https://doi.org/10.1016/J.AGRFORMET.2018.11.012

Dinno A. (2017) *Package 'dunn.test'*. CRAN Repository 1–7. R Foundation for Statistical Computing, Vienna, Austria.

Dolos K., Märkel U. (2016) Modellierung der klimatischen Standorteignung forstlich relevanter Baumarten. *LUBW KLIMOPASS-Berichte*.

Eilmann B., Zweifel R., Buchmann N., Fonti P., Rigling A. (2009) Drought-induced adaptation of the xylem in Scots pine and pubescent oak. *Tree Physiology*, **29**, 1011–1020. https://doi.org/10.1093/treephys/tpp035

Eilmann B., Zweifel R., Buchmann N., Graf Pannatier E., Rigling A. (2011) Drought alters timing, quantity, and quality of wood formation in Scots pine. *Journal of Experimental Botany*, **62**, 2763–2771. https://doi.org/10.1093/jxb/erq443

Federer C.A., Vörösmarty C., Fekete B. (2003) Sensitivity of annual evaporation to soil and root properties in two models of contrasting complexity. *Journal of Hydrometeorology*, **4**, 1276–1290.

Fonti P., von Arx G., García-González I., Eilmann B., Sass-Klaassen U., Gärtner H., Eckstein D. (2010) Studying global change through investigation of the plastic responses of xylem anatomy in tree rings. *New Phytologist*, **185**, 42–53. https://doi.org/10.1111/j.1469-8137.2009.03030.x

Fromm J. (2013) *Cellular aspects of wood formation*. Springer, Berlin, Germany.

Füssel H.-M., Jol A., Marx A., Hildén M. (2017) *Climate change, impacts and vulnerability in Europe 2016*. European Environment Agency, Copenhagen, Denmark.

Garcia-Forner N., Vieira J., Nabais C., Carvalho A., Martínez-Vilalta J., Campelo F. (2019) Climatic and physiological regulation of the bimodal xylem formation pattern in *Pinus pinaster* saplings. *Tree Physiology*, **39**(12), 2008–2018. https://doi.org/10.1093/treephys/tpz099

Gärtner H., Lucchinetti S., Schweingruber F.H. (2014) New perspectives for wood anatomical analysis in dendrosciences: the GSL1-microtome. *Dendrochronologia*, **32**, 47–51. https://doi.org/10.1016/j.dendro.2013.07.002

van Genuchten M.T. (1980) A closed-form equation for predicting the hydraulic conductivity of unsaturated soils. *Soil Science Society of America Journal*, **44**, 892–898.

George J.-P., Schueler S., Karanitsch-Ackerl S., Mayer K., Klumpp R.T., Grabner M. (2015) Inter- and intra-specific variation in drought sensitivity in *Abies* spec. and its relation to wood density and growth traits. *Agricultural and Forest Meteorology*, **214–215**, 430–443. https://doi.org/10.1016/j.agrformet.2015.08.268

Gessler A., Grossiord C. (2019) Coordinating supply and demand: plant carbon allocation strategy ensuring survival in the long run. *New Phytologist*, **222**, 5–7. https://doi.org/10.1111/nph.15583

Gruber A., Strobl S., Veit B., Oberhuber W. (2010) Impact of drought on the temporal dynamics of wood formation in *Pinus sylvestris*. *Tree Physiology*, **30**(4), 490–501. https://doi.org/10.1093/treephys/tpq003

Hacke U.G., Sperry J.S. (2001) Functional and ecological xylem anatomy. *Perspectives in Plant Ecology, Evolution and Systematics*, **4**, 97–115.

Hammel K., Kennel M. (2001) *Charakterisierung und Analyse der Wasserverfügbarkeit und des Wasserhaushalts von Waldstandorten in Bayern mit dem Simulationsmodell BROOK90*. Frank.

Hilty J., Muller B., Florent P., Leuzinger S. (2021) Plant growth: the what, the how, and the why. *New Phytologist*, 232(1), 25–41. https://doi.org/10.1111/nph.17610

Ionita M., Nagavciuc V. (2021) Changes in drought features at European level over the last 120 years. *Natural Hazards and Earth System Sciences*, 1–31. https://doi.org/10.5194/nhess-2021-46

Jyske T., Mäkinen H., Kalliokoski T., Nöjd P. (2014) Intra-annual tracheid production of Norway spruce and Scots pine across a latitudinal gradient in Finland. *Agricultural and Forest Meteorology*, 194, 241–254. https://doi.org/10.1016/j.agrformet.2014.04.015

Körner C. (2003) Carbon limitation in trees. *Journal of Ecology*, 91, 4–17. https://doi.org/10.1046/j.1365-2745.2003.00742.x

Lamlom S.H., Savidge R.A. (2003) A reassessment of carbon content in wood: variation within and between 41 North American species. *Biomass and Bioenergy*, 25, 381–388. https://doi.org/10.1016/S0961-9534(03)00033-3

Larysch E., Stangler D.F., Nazari M., Seifert T., Kahle H.-P. (2021) Xylem phenology and growth response of European beech, silver fir and scots pine along an elevational gradient during the extreme drought year 2018. *Forests*, 12, 75. https://doi.org/10.3390/f12010075

Lebourgeois F., Rathgeber C.B.K., Ulrich E. (2010) Sensitivity of French temperate coniferous forests to climate variability and extreme events (*Abies alba*, *Picea abies* and *Pinus sylvestris*). *Journal of Vegetation Science*, 21, 364–376. https://doi.org/10.1111/j.1654-1103.2009.01148.x

Lindner M., Verkerk H. (2020) *Question 4 How has climate change affected EU forests and what might happen next?*. European Forest Institute, Joensuu, Finland.

van der Maaten-Theunissen M., Kahle H.-P., van der Maaten E. (2013) Drought sensitivity of Norway spruce is higher than that of silver fir along an altitudinal gradient in southwestern Germany. *Annals of Forest Science*, 70, 185–193. https://doi.org/10.1007/s13595-012-0241-0

Martin-Benito D., Anchukaitis K., Evans M., del Río M., Beeckman H., Cañellas I. (2017) Effects of drought on xylem anatomy and water-use efficiency of two co-occurring pine species. *Forests*, 8, 332. https://doi.org/10.3390/f8090332

Martinez del Castillo E., Prislan P., Gričar J., Gryc V., Merela M., Giagli K., de Luis M., Vavrčík H., Čufar K. (2018) Challenges for growth of beech and co-occurring conifers in a changing climate context. *Dendrochronologia*, 52, 1–10. https://doi.org/10.1016/j.dendro.2018.09.001

Meining S., Puhlmann H., Augustin N. (2016) *Waldzustandsbericht 2016 für Baden-Württemberg*. Forstliche Versuchs- und Forschungsanstalt Baden-Württemberg (FVA), Germany.

Messier C., Bauhus J., Sousa-Silva R., Auge H., Baeten L., Barsoum N., Bruelheide H., Caldwell B., Cavender-Bares J., Dhiedt E., Eisenhauer N., Ganade G., Gravel D., Guillemot J., Hall J.S., Hector A., Hérault B., Jactel H., Koricheva J., Kreft H., Mereu S., Muys B., Nock C.A., Paquette A., Parker J.D., Perring M.P., Ponette Q., Potvin C., Reich P.B., Scherer-Lorenzen M., Schnabel F., Verheyen K., Weih M., Wollni M., Zemp D.C. (2021) For the sake of resilience and multifunctionality, let's diversify planted forests! *Conservation Letters*, 1–8. https://doi.org/10.1111/conl.12829

Miller T.W., Stangler D.F., Larysch E., Seifert T., Spiecker H., Kahle H.-P. (2020) Plasticity of seasonal xylem and phloem production of Norway spruce along an elevational gradient. *Trees*, 34, 1281–1297. https://doi.org/10.1007/s00468-020-01997-6

Montwé D., Spiecker H., Hamann A. (2014) An experimentally controlled extreme drought in a Norway spruce forest reveals fast hydraulic response and subsequent recovery of growth rates. *Trees*, 28, 891–900. https://doi.org/10.1007/s00468-014-1002-5

Mualem Y. (1976) A new model for predicting the hydraulic conductivity of unsaturated porous media. *Water Resources Research*, 12, 513–522.

Nabais C., Campelo F., Vieira J., Cherubini P. (2014) Climatic signals of tree-ring width and intra-annual density fluctuations in *Pinus pinaster* and *Pinus pinea* along a latitudinal gradient in Portugal. *Forestry*, 87, 598–605. https://doi.org/10.1093/forestry/cpu021

Oberhuber W., Stumböck M., Kofler W. (1998) Climate–tree–growth relationships of Scots pine stands (*Pinus sylvestris* L.) exposed to soil dryness. *Trees*, 13, 19–27. https://doi.org/10.1007/s004680050183

Pacheco A., Camarero J.J., Ribas M., Gazol A., Gutierrez E., Carrer M. (2018) Disentangling the climate-driven bimodal growth pattern in coastal and continental Mediterranean pine stands. *Science of the Total Environment*, 615, 1518–1526. https://doi.org/10.1016/j.scitotenv.2017.09.133

Pan Y., Birdsey R.A., Fang J., Houghton R., Kauppi P.E., Kurz W.A., Phillips O.L., Shvidenko A., Lewis S.L., Canadell J.G., Ciais P., Jackson R.B., Pacala S.W., McGuire A.D., Piao S., Rautiainen A., Sitch S., Hayes D. (2011) A large and persistent carbon sink in the world's forests. *Science*, 333(6045), 988–993.

Pantin F., Fanciullino A.-L., Massonnet C., Dauzat M., Simonneau T., Muller B. (2013) Buffering growth variations against water deficits through timely carbon usage. *Frontiers in Plant Science*, 4, 1–11. https://doi.org/10.3389/fpls.2013.00483

Peters R.L., Balanzategui D., Hurley A.G., von Arx G., Prendin A.L., Cuny H.E., Björklund J., Frank D.C., Fonti P. (2018) RAPTOR: row and position tracheid organizer in R. *Dendrochronologia*, 47, 10–16. https://doi.org/10.1016/j.dendro.2017.10.003

Peters R.L., Steppe K., Cuny H.E., De Pauw D.J.W., Frank D.C., Schaub M., Rathgeber C.B.K., Cabon A., Fonti P. (2021) Turgor—a limiting factor for radial growth in mature conifers along an elevational gradient. *New Phytologist*, 229, 213–229. https://doi.org/10.1111/nph.16872

Prendin A.L., Petit G., Carrer M., Fonti P., Björklund J., von Arx G. (2017) New research perspectives from a novel approach to quantify tracheid wall thickness. *Tree Physiology*, 37, 976–983. https://doi.org/10.1093/treephys/tpx037

R Core Team (2019) *R Programming Language*. R Foundation for Statistical Computing, Vienna, Austria. www.r-project.org

Rathgeber C.B.K., Cuny H.E., Fonti P. (2016) Biological basis of tree-ring formation: a crash course. *Frontiers in Plant Science*, 7. https://doi.org/10.3389/fpls.2016.00734

Rathgeber C.B.K., Fonti P., Shishov V. V., Rozenberg P. (2019) Wood formation and tree adaptation to climate. *Annals of Forest Science*, 76, 10–12. https://doi.org/10.1007/s13595-019-0902-3

Reif A., Brucker U., Kratzer R., Schmiedinger, A. & Bauhus, J. (2010) Waldbau und Baumartenwahl in Zeiten des Klimawandels aus Sicht des Naturschutzes. *BfN-Skripten*, 272, 125.

Ren P., Rossi S., Gricar J., Liang E., Cufar K. (2015) Is precipitation a trigger for the onset of xylogenesis in *Juniperus przewalskii* on the north-eastern Tibetan Plateau? *Annals of Botany*, 115, 629–639. https://doi.org/10.1093/aob/mcu259

Rossi S., Anfodillo T., Menardi R. (2006) Trephor: a new tool for sampling microcores from tree stems. *IAWA Journal*, 27, 89–97.

Rossi S., Deslauriers A., Griçar J., Seo J.-W., Rathgeber C.B.K., Anfodillo T., Morin H., Levanic T., Oven P., Jalkanen R. (2008) Critical temperatures for xylogenesis in conifers of cold climates. *Global Ecology and Biogeography*, 17, 696–707. https://doi.org/10.1111/j.1466-8238.2008.00417.x

Saderi S., Rathgeber C.B.K., Rozenberg P., Fournier M. (2019) Phenology of wood formation in larch (*Larix decidua* Mill.) trees growing along a 1000-m elevation gradient in the French Southern Alps. *Annals of Forest Science*, 76(3). https://doi.org/10.1007/s13595-019-0866-3

Schuldt B., Buras A., Arend M., Vitasse Y., Beierkuhnlein C., Damm A., Gharun M., Grams T.E.E., Hauck M., Hajek P., Hartmann H., Hiltbrunner E., Hoch G., Holloway-Phillips M., Körner C., Larysch E., Lübbe T., Nelson D.B., Rammig A., Rigling A., Rose L., Ruehr N.K., Schumann K., Weiser F., Werner C., Wohlgemuth T., Zang C.S., Kahmen A. (2020) A first assessment of the impact of the extreme 2018 summer drought on Central European forests. *Basic and Applied Ecology*, 45, 86–103. https://doi.org/10.1016/j.baae.2020.04.003

Seneviratne S.I., Zhang X., Adnan M., Badi, W., Dereczynski, C., Di Luca, A., Ghosh, S., Iskandar, I., Kossin, J., Lewis, S., Otto, F., Pinto, I., Satoh, M., Vicente-Serrano, S.M., Wehner, M., Zhou, B. (2021) Weather and Climate Extreme Events in a Changing Climate. In: Climate change 2021: the physical science basis. Contribution of Working Group I to the Sixth Assessment Report of the Intergovernmental Panel on Climate Change.

Shuttleworth W.J., Wallace J.S. (1985) Evaporation from sparse crops—an energy combination theory. *Quarterly Journal of the Royal Meteorological Society*, 111, 839–855.

Simard S., Giovannelli A., Treydte K., Traversi M.L., King G.M., Frank D., Fonti P. (2013) Intra-annual dynamics of non-structural carbohydrates in the cambium of mature conifer trees reflects radial growth demands. *Tree Physiology*, 33, 913–923. https://doi.org/10.1093/treephys/tpt075

Stangler D.F., Kahle H.-P., Raden M., Larysch E., Seifert T., Spiecker H. (2021) Effects of intra-seasonal drought on kinetics of tracheid differentiation and seasonal growth dynamics of Norway Spruce along an elevational gradient. *Forests*, 12, 274. https://doi.org/10.3390/f12030274

Steppe K., de Pauw D.J.W., Lemeur R., Vanrolleghem P.A. (2006) A mathematical model linking tree sap flow dynamics to daily stem diameter fluctuations and radial stem growth. *Tree Physiology*, 26, 257–273. https://doi.org/10.1093/treephys/26.3.257

Thomas S.C., Martin A.R. (2012) Carbon content of tree tissues: a synthesis. *Forests*, 3, 332–352. https://doi.org/10.3390/f3020332

Torrey J.G., Fosket D.E., Hepler P.K. (1971) Xylem formation: a paradigm of cytodifferentiation in higher plants. *American Scientist*, 59, 338–352.

Vanhellemont M., Sousa-Silva R., Maes S.L., Van den Bulcke J., Hertzog L., De Groote S.R.E., Van Acker J., Bonte D., Martel A.N., Lens L., Verheyen K. (2019) Distinct growth responses to drought for oak and beech in temperate mixed forests. *Science of the Total Environment*, **650**, 3017–3026. https://doi.org/10.1016/J.SCITOTENV.2018.10.054

Vanoni M., Bugmann H., Nötzli M., Bigler C. (2016) Drought and frost contribute to abrupt growth decreases before tree mortality in nine temperate tree species. *Forest Ecology and Management*, **382**, 51–63.

Vieira J., Carvalho A., Campelo F. (2020) Tree growth under climate change: evidence from xylogenesis timings and kinetics. *Frontiers in Plant Science*, **11**, 1–11. https://doi.org/10.3389/fpls.2020.00090

Vieira J., Moura M., Nabais C., Freitas H., Campelo F. (2019) Seasonal adjustment of primary and secondary growth in maritime pine under simulated climatic changes. *Annals of Forest Science*, **76**. https://doi.org/10.1007/s13595-019-0865-4

Vieira J., Rossi S., Campelo F., Freitas H., Nabais C. (2013) Seasonal and daily cycles of stem radial variation of *Pinus pinaster* in a drought-prone environment. *Agricultural and Forest Meteorology*, **180**, 173–181. https://doi.org/10.1016/j.agrformet.2013.06.009

Weemstra M., Eilmann B., Sass-Klaassen U., Sterck F.J. (2013) Summer droughts limit tree growth across 10 temperate species on a productive forest site. *Forest Ecology and Management*, **306**, 142–149. https://doi.org/10.1016/j.foreco.2013.06.007

Wood S.N. (2017) *Generalized additive models*. Chapman and Hall/CRC Press, London, UK.

Yin J., Bauerle T.L. (2017) A global analysis of plant recovery performance from water stress. *Oikos*, **126** (10), 1377–1388. https://doi.org/10.1111/oik.04534

Zhao M., Running S.W. (2010) Drought-induced reduction in global terrestrial net primary production from 2000 through 2009. *Science*, **329**, 940–943. https://doi.org/10.1126/science.1192666